Accepted Manuscript

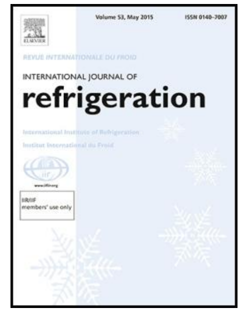

Title: Performance analysis of a r744 ground source heat pump system with air-cooled and water-cooled gas coolers

Author: Haitao Hu, Trygve Magne Eikevik, Petter Neksa, Armin Hafner, Guoliang Ding, Qingnan Huang, Jingjing Ye

PII: S0140-7007(15)00324-2
DOI: http://dx.doi.org/doi: 10.1016/j.ijrefrig.2015.10.029
Reference: JIJR 3185

To appear in: *International Journal of Refrigeration*

Received date: 30-6-2015
Revised date: 21-9-2015
Accepted date: 27-10-2015

Performance analysis of a R744 ground source heat pump system with air-cooled and water-cooled gas coolers

Haitao Hu[a,b,*], Trygve Magne Eikevik[b], Petter Neksa[c], Armin Hafner[c], Guoliang Ding[a], Qingnan Huang[a], Jingjing Ye[a]

([a] Shanghai Jiao Tong University, 800 Dongchuan Road, 200240, Shanghai, China;

[b] Norwegian University of Science and Technology, Kolbjorn Hejes vei 1B, NO-7491 Trondheim, Norway;

[c] SINTEF Energy Research, Kolbjorn Hejes vei 1D, NO-7465 Trondheim, Norway)

* Corresponding Author, Tel: 86-21-34206295; Fax: 86-21-34206295; E-mail: huhaitao2001@sjtu.edu.cn

Highlights

- A R744 GSHP system with air-cooled and water-cooled gas coolers was designed.
- Earth's energy imbalance degree for the proposed R744 system was analyzed.
- Investment and operation costs of the R744 system were decreased.
- Effect of ground heat exchanger depth on system performance was analyzed.

Abstract:

In order to decrease the earth's energy imbalance degree, a R744 ground source heat pump system (GSHPS) with air-cooled and water-cooled gas coolers was designed, and the performances of this system were analyzed numerically. The results show that, for the proposed R744 system in different regions, the earth's energy imbalance degree can always be decreased to zero by optimizing the cooling load proportion of air-cooled gas cooler. Comparing with the system without air-cooled gas cooler, the investment cost of the proposed R744 system is decreased by 14.5%~25.5% due to the decreasing cost of ground heat exchanger, and the coefficient of performance is increased. With the increase of ground heat exchanger depth, the performance deteriorates, and the ground heat exchanger with shorter depth is preferred in the GSHPS. The investment and operation costs of the proposed R744 system are lower than that of the existing R134a system.

Keywords: Energy imbalance degree; Gas cooler; Ground source heat exchanger; Heat pump; R744

1. Introduction

The rapid increase of the global energy consumption aggravates the energy shortage and environmental pollution (Omer, 2008). Among the global energy consumption, more than twenty percent of the energy demand is consumed by the air-conditioning and heat pump systems, and this proportion is even larger in hot-weather areas (Man et al., 2010). Heat pumps present a significant advantage over the conventional residential heating technologies due to higher energy efficiencies (Shen et al., 2012; Abdelaziz and Shen, 2012; Abdelaziz et al., 2011). In order to decrease the energy consumption of the air-conditioning and heat pump systems, the ground source heat pump (GSHP) technology has been widely applied and showed a trend of booming growth in different countries (Yuan et al., 2012, Bayer et al., 2012, Bakirci et al., 2012, Tarnawski et al., 2009, Capozza et al., 2012, Sagia et al., 2012, Aikins et al., 2012 and Liu et al., 2009). The worldwide installed capacity of GSHPs is about 33 GWt and the annual energy use of GSHPs is over 55 TWh; the number of countries with installation increased from 26 in 2000, to 33 in 2005, and to 43 in 2010 (Madani et al., 2013, Lunda et al., 2011). The most important influence factor for the GSHP systems is the imbalance degree of the earth energy. When GSHP systems are installed in the moderate-climate regions, the coefficient of performance (COP) of GSHP systems was 20%~30% higher than those of conventional air source heat pump (ASHP) systems (Man et al., 2010); while when GSHP systems are used in the cooling-dominated buildings in hot climates, the heat buildup within the ground will definitely increase the ground temperature and deteriorate the system performance over time (Man et al., 2010, Zhang and Wei, 2012 and Yang et al., 2010). Therefore, new methods are needed to decrease the imbalance degree of the earth energy for the GSHP systems.

In the past decades, the most of geothermal hybrid heat pump systems in the world have used R22 as a refrigerant and it still has big portion for use (Choi et al., 2014). Refrigerant regulations have been tightened and expanded by various organizations because chlorofluorocarbon (CFC) and hydrochlorofluorocarbon (HCFC) refrigerants have added to environmental problems such as ozone depletion and global warming (Choi et al., 2014). CO_2 (i.e. R744) is a natural substance with a low GWP and zero impact on the ozone layer (Ge and Cropper, 2009 and Nekså, 2002), and it has a high heat transfer performance, making CO_2 attract more and more attention in the refrigeration and heat pump applications (Richter et al., 2003, Cavallini et al., 2005, Oritz et al., 2003, Xu et al., 2012, Dai et al., 2014 and Li et al., 2015).

An inverse R744 operated cycle is much different from a traditional one, since the high pressure is often supercritical and the refrigeration cycle does not entail condensation, but a simple cooling process of dense fluid accomplished in the so-called 'gas cooler' (Wang et al., 2013). Unlike a conventional sub-critical refrigeration cycle, the transcritical cycle does not suffer capacity and efficiency losses at high heat rejection temperatures (Austin and Sumathy, 2011a), which promotes the application of R744 system in hot climates. The heat transfer characteristics of supercritical R744 flow in tubes were investigated (Dang and Hihara, 2012, Jiang et al., 2008, Zhang and Yamaguchi, 2007 and Yang et al, 2013), and the performances of R744 transcritical cycles were discussed and optimized (Richter et al., 2003, Cavallini et al., 2005, Oritz et al., 2003, Xu et al., 2012 and Dai et al., 2014). However, there is limited literature on R744 ground source heat pumps. Therefore, the investigation on the performance of R744 GSHP system is necessary for optimizing the system to decrease the imbalance degree of the earth energy.

For R744 GSHP system, the existing research mainly focuses on the solar-geothermal hybrid heat pumps (Choi et al., 2014) and the direct-expansion R744 geothermal heat pump (Austin and Sumathy, 2011a). For the solar-geothermal hybrid heat pumps (Choi et al., 2014), the efficiency of the solar collector in R744 solar-geothermal hybrid heat pump is 4.1% higher than that in R22 one, and the heating capacity of the R22 heat pump was 10% higher than that of the R744 heat pump; the solar collector system was more effective in the R744 hybrid heat pump compared to that in the R22 hybrid heat pump. For the direct-expansion R744 geothermal heat pump (Austin and Sumathy, 2011a), the refrigerant flows inside the horizontal ground source heat exchanger to exchange heat with the ground, and the direct-expansion R744 geothermal system could achieve a coefficient of performance of 2.58, representing an 18% improvement compared to the baseline system (Austin and Sumathy, 2011a). The adopted horizontal ground source heat changer is suitable for small buildings, but not suitable for the big buildings in megacities (Yang et al., 2013). For the direct-expansion R744 geothermal heat pump, the earth energy is imbalanced because the ground heat exchanger does not release the heat but only extracts the heat from the earth.

For the GSHP system using conventional refrigerants, the main existing methods to decrease the imbalance degree of earth energy for GSHP systems are using hybrid ground source heat pump system, e.g. the utilization of solar energy or other thermal energy in heating-dominated buildings (Bi et al., 2004, Wang et al., 2009, Rad et al., 2013, Bakirci et al., 2011, Ozgener and Hepbasli, 2007, Ozgener and Hepbasli, 2005a, Ozgener and Hepbasli, 2005b, Si et al., 2014, Han et al., 2008 and Qi et al., 2014) and cooling towers in cooling-dominated buildings (Man et al., 2010, Zhai et al., 2011, Sagia et al., 2012, Jeon et al., 2010). For the heating-dominated buildings, the feasibility of solar-ground source heat pump system was validated for the buildings in Canada (Rad et al., 2013), Turkey (Ozgener and Hepbasli, 2007, Ozgener and Hepbasli, 2005a and Ozgener and Hepbasli, 2005b), China (Bi et al., 2004, Si et al., 2014, Han et al., 2008 and Qi et al., 2014) and other countries (Qi et al., 2014), and the solar thermal energy storage could reduce the ground heat exchanger (GHX) length (Rad et al., 2013 and Bakirci et al., 2011). For the cooling-dominated buildings, the hybrid ground source heat pump systems with the cooling tower (Sagia et al., 2012) or water chiller (Jeon et al., 2010) are normally used, and the optimal operation strategies were proposed (Alavy et al., 2013, Wang et al., 2012 and Hackel and Pertzborn, 2011). However, for the hybrid ground source heat pump systems, the added complexity leads to the technical challenges that have slowed the growth of the hybrid approach (Hackel and Pertzborn, 2011). Recently, another effective method to efficiently use the energy instead of the hybrid systems was proposed by adopting heat recovery technologies (Zhai et al., 2012), and the imbalance degree of the earth energy for the system can be decreased by 33.7% (Zhai et al., 2012, Zhai and Yang, 2011, Yu et al., 2010a and Yu et al., 2010b). In the above existing researches, the refrigerants are conventional refrigerants. Due to the different cycle performances between R744 system and the conventional refrigerant systems, the existing research results on the conventional refrigerant systems can not be directly extended to those on R744 system.

In order to decrease the imbalance degree of the R744 GSHP system, a transcritical cycle with the ambient air-cooled and water-cooled gas coolers can be used. For the conventional subcritical refrigeration cycle (Fig. 1(a)), the system performance will be decreased significantly as the environmental temperature is very high (Ma et al., 2013); while for the transcritical cycle (Fig. 1(b)), there is a great temperature drop during the R744 cooled process in the critical region, and a special Lorentz cycle can be formed, resulting in a good system efficiency (Austin and Sumathy, 2011b and Ma et al., 2013). In the high temperature environment, a large part of heat can still be released to the ambient by the ambient air-cooled gas cooler, resulting in a better performance of the R744 system than that of the conventional refrigerant systems. Therefore, using R744 GSHP system coupled with the ambient air-cooled gas cooler and water-cooled gas cooler is one good way to decrease the imbalance degree of the earth energy by releasing a portion of the heat load to the ambient air instead of the ground.

In the present study, the performance of a R744 GSHP system with an ambient air-cooled gas cooler and a water-cooled gas cooler will be analyzed for different climates, and the influencing factors will be analyzed to decrease the earth's energy imbalance degree.

2. Description on the R744 GSHP system with air-cooled and water-cooled gas coolers

2.1 Structure configuration and operation principle of the proposed 744 GSHP system with air-cooled and water-cooled gas coolers

A R744 GSHP system with the air-cooled and water-cooled gas coolers was developed for different climates, as shown in Fig. 2. The major components in the system include a vertical ground heat exchanger (VGHX), an air handling unit (AHU), and a heat pump with the air-cooled and water-cooled gas coolers. The air-cooled gas cooler is a fin-tube heat exchanger, and the water-cooled gas cooler is a tube-in-tube heat exchanger; in the water-cooled tube-in-tube heat exchanger, the supercritical R744 flows in the inner tube, and the water from the VGHX flows in the annulus to cool down the R744; the AHU was designed to connect with the water loop in order to decrease the refrigerant charge amount in the system. All the components were connected by tubes and valves to form the whole circulating system.

The system consists of three loops: a refrigerant loop, a water loop connected with the VGHX, and a water loop connected with the AHU. In the refrigerant loop, the circulation fluid is R744. The supercritical R744 from the compressor is separated into two parallel passes: a portion of refrigerant passes through the ambient air cooled-gas cooler and the water-cooled gas cooler in turn, and the other part of refrigerant directly flows into the water-cooled gas cooler. The cooled refrigerant out of the water-cooled gas cooler passes through an electronic expansion valve. Then it flows through the shell-and-tube evaporator and is fully evaporated and then superheated. The superheated vapor refrigerant enters into the suction inlet of the compressor. In the water loop connected with the VGHX, the water pumped out from the VGHX enters into the water-cooled gas cooler or the evaporator. In the water loop connected with the AHU, the water from the AHU also enters into the water-cooled gas cooler or the evaporator. The water flow direction can be adjusted to meet the cooling or heating load of the building according to the climates.

The system was designed for keeping the temperature as a constant for the archives building. Archives are places containing records, documents, or other materials of historical interest; there are always priceless collections of papers, portraits and photographs in such buildings (Zhai and Yang, 2011). Consequently, maintaining high quality air-conditioning is vital to avoid damage to the works of art. For the archives building, the indoor temperature should be controlled as a constant, which is within 19 ^{o}C ~ 24 ^{o}C (Zhai and Yang, 2011). When the indoor temperature of the archives building is higher than the setting temperature, the cooling mode of the system starts; while when the indoor temperature of the archives building is lower than the setting temperature, the heating mode of the system starts. Through the valves located on the pipes, the system can be switched to different operating modes according to different seasons.

Under the cooling mode, the valves 5, 6, 17 and 18 are closed, while the valves 7, 8, 15 and 16 are opened. Thereby, the evaporator of the heat pump system is connected with the cooling coil of the AHU to provide the cooling capacity for the building; the refrigerant R744 coming from the compressor enters into the air-cooled gas cooler to release the heat to the environment, and then enters into the water-cooled gas cooler to release the heat to the water circulated in the ground source heat exchanger. The supercritical refrigerant from compressor is cooled by the air firstly and then is cooled by the water circulating in the ground heat exchanger. Therefore, the cooling capacity of the gas cooler can be shared by the air and the water.

Under the heating mode, the valves 7, 8, 15 and 16 are closed, while the valves 5, 6, 17 and 18 are opened; in addition, the valves 11 and 12 are closed. Thereby, the evaporator is connected with the ground heat exchanger, and the water-cooled gas cooler is connected with the heating coil of the AHU to provide the heating load demand for the building.

The detail control method of air-cooled and water-cooled gas coolers are explained as below. The air-cooled gas cooler operates only under the cooling mode, and it will be turned on when the environmental temperature is higher than the setting start-up temperature of air-cooled gas cooler. For different climates, the ambient temperature and the whole year climatic conditions were output by the software of METEONORM (2006), and then were used to drive the simulation in TRNSYS 17.1 software (2012) to obtain the whole year cooling and heating loads of the building in different climates. The energy loads for different climates were integrated with the mathematic model of the proposed R744 system. The optimized air cooling load proportion corresponding to the earth's energy balance condition can be calculated, and then the optimized setting start-up temperature of air-cooled gas cooler can be obtained. If the environmental temperature is lower than the setting start-up temperature, only the water-cooled gas cooler operates; if the environmental temperature is higher than the setting start-up temperature, the air-cooled gas cooler starts to operate.

2.2 Main performance indexes for R744 GSHP system with air-cooled and water-cooled gas coolers

The proposed R744 GSHP system with the air-cooled and water-cooled gas coolers can be optimized by adjusting the cooling load proportion of the air-cooled gas cooler to increase the system performance coefficient, to decrease the system investment and operation costs, and to decrease the earth's energy imbalance degree.

The coefficient of performance of the system is expressed as the ratio of the cooling and heating capacities for the building to the power consumption of the GSHP system:

$$OP_{sys} = \frac{\sum(Q_{cooling}+Q_{heating})}{\sum W} \tag{1}$$

$$Q_{cooling} = m_{w,e}Cp_w\left(T_{o,e} - T_{i,e}\right) \tag{2}$$

$$Q_{heating} = m_{w,c}Cp_w(T_{o,GC} - T_{i,GC}) \tag{3}$$

where, $Q_{cooling}$ and $Q_{heating}$ are the cooling and heating capacities of the building, respectively.

The investment cost of the system is equal to the sum of the investment costs of all of the components, the connecting tubes and the valves, as shown in Eq. (4); the operating cost of the system is equal to the sum of electrical power costs of different components, including the electrical power of fans, compressor and pumps, as shown in Eq. (5).

$$ost_{inv} = \sum(\ ost_{com} + \ ost_{GC} + \ ost_{Eva} + \ ost_{GHX} + \ ost_{Tube} + \ ost_{Vavle}) \tag{4}$$

$$ost_{Oper} = \sum \ ost_{Electric} \tag{5}$$

Air cooling load proportion is defined as the ratio of the cooling capacity of the air-cooled gas cooler ($Q_{cooling,AGC}$) to the total cooling capacity of the air-cooled and water-cooled gas coolers in the system ($Q_{cooling,tot}$), as shown in Eq. (6). The earth's energy imbalance degree is defined as the ratio of the heat energy discharged to the ground ($Q_{GHX,dis}$) to that extracted from the ground ($Q_{GHX,ext}$), as shown in Eq. (7)

$$\varphi_{Air,cooling} = \frac{Q_{cooling,AGC}}{Q_{cooling,tot}} \tag{6}$$

$$\Delta E_{un} = \frac{Q_{GHX,dis} - Q_{GHX,ext}}{\max(Q_{GHX,dis}, Q_{GHX,ext})} \times 100\%$$

$$= \frac{Q_{cooling} + W_{Summer} - (Q_{heating} - W_{winter})}{\max(Q_{GHX,dis}, Q_{GHX,ext})} \times 100\% \tag{7}$$

where, w_{summer} and w_{winter} are the power consumption of the R744 GSHP system in summer and winter, respectively.

In order to quantitatively evaluate the system performance, the simulation models of ground heat exchanger and heat pump system should be developed, as shown below.

3 Mathematic model of R744 GSHP system with air-cooled and water-cooled gas coolers

3.1 Model of ground heat exchanger

The model of ground heat exchanger is transient, and the performance of ground heat exchanger varies with the changes of the temperature distributions of the soil around the heat exchanger and the water inside the heat exchanger.

The temperature distribution of the soil around the U-tube ground heat exchanger is calculated by the following equation:

$$\frac{\partial T_g}{\partial \tau} = \alpha_g \left(\frac{\partial^2 T_g}{\partial x^2} + \frac{1}{x} \frac{\partial T_g}{\partial x} \right) \tag{8}$$

where, T_g is the soil temperature, α_g is the thermal diffusivity of soil, τ is the time, and x is the distance to the borehole center.

The heat transfer between the ground heat exchanger and the soil is calculated by:

$$Q_{GX} = m_{w,GX} Cp_{w,GX} \left| T_{in,GX} - T_{out,GX} \right| \tag{9}$$

The temperature distributions of the water in the inlet and outlet U-tubes are given by Eqs. (10) and (11), respectively (Zeng et al., 2002 and Zeng et al., 2003):

$$\theta(Z) = \cos h(\beta Z) - \frac{1}{\sqrt{1-P^2}} \times \left[1 - P \frac{\cos h(\beta) - \sqrt{\frac{1-P}{1+P}} \sin h(\beta Z)}{\cos h(\beta) + \sqrt{\frac{1-P}{1+P}} \sin h(\beta Z)} \right] \sin h(\beta Z) \tag{10}$$

$$\theta(Z) = \frac{\cos h(\beta) - \sqrt{\frac{1-P}{1+P}} \sin h(\beta)}{\cos h(\beta) + \sqrt{\frac{1-P}{1+P}} \sin h(\beta)} \cos h(\beta Z) + \frac{1}{\sqrt{1-P^2}} \times \left[P \frac{\cos h(\beta) - \sqrt{\frac{1-P}{1+P}} \sin h(\beta Z)}{\cos h(\beta) + \sqrt{\frac{1-P}{1+P}} \sin h(\beta Z)} - P \right] \sin h(\beta Z) \tag{11}$$

$$\beta = \frac{H}{m_W Cp_{W\sqrt{(R_{11}+R_{12})(R_{11}-R_{12})}}} \tag{12}$$

where, θ, Z and P are the nondimensional temperature, length and thermal resistance (Zeng et al., 2002 and Zeng et al., 2003), respectively; m_W and Cp_W are the mass flow rate and the specific heat of water inside tube, respectively.

3.2 Model of gas cooler

For the air-cooled gas cooler, the performances can be predicted by the generalized heat transfer and frictional correlation proposed by Wang et al. (1999), which will be verified by the experimental data of the ambient air-cooled gas cooler in Section 3.4.

For the water-cooled gas cooler, it is a counter-flow, concentric tube heat exchanger with R744 flowing in the inner-tube and water flowing through the annular tube. Figure 3 represents one element of the water-cooled gas cooler. Properties are assumed to be constant throughout the control volume element. Outlet conditions for one element are calculated, and these become the inlet conditions for the next element. The overall gas cooler analysis is then carried out by successively calculating the pressure drop, temperature change and the heat transfer rate in each element.

For each control volume segment shown in Fig. 3, the energy gained by water must be equal to the energy rejected by R744 (Austin and Sumathy, 2011a). Thus the energy balance equations can be equated as follows:

$$\dot{Q}^i = \dot{m}_w c_{\mathrm{p,w}} \left(T_w^i - T_w^{i+1} \right) = \dot{m}_w c_{\mathrm{p,c}} \left(T_c^i - T_c^{i+1} \right) \tag{13}$$

$$\dot{Q}^i = \varepsilon C \min \left(T_c^i - T_w^{i+1} \right) \tag{14}$$

$$\varepsilon = \frac{1 - \exp\left[-NTU\,(1-R) \right]}{1 - C \times \exp\left[-NTU\,(1-R) \right]}, NTU = \frac{UA}{C\min}, R = \frac{C\min}{C\max} \tag{15}$$

In Eq. (14), the overall heat transfer coefficient (*UA*) is obtained as the sum of the resistivity values, including the convective resistance of R744, the conductive resistance of tube-wall and the convective resistance of the water (Austin and Sumathy, 2011a). The water inlet temperature of the water-cooled gas cooler is the same as the outlet water temperature of the ground heat exchanger, which is calculated by Eq. (10).

3.3 Model of heat pump system

For the compressor, the model is steady-state, and the power depends on the R744 mass flow rate, the total efficiency and the isentropic change in R744 enthalpy:

$$\dot{W}_{\mathrm{comp}} = \frac{\dot{m}_c \left(h_{2,\mathrm{isen}} - h_1 \right)}{\eta_{\mathrm{tot}}} \tag{16}$$

$$\dot{m} = V_{\mathrm{S}} \cdot \eta_{\mathrm{vol}} \cdot N \cdot \rho_1 \tag{17}$$

where, V_{S} is the swept volume, N is the compressor speed and ρ_1 is the suction density; η_{tot} and η_{vol} are the compressor's total efficiency and the volumetric efficiency, respectively, which is assumed to correspond with Oritz et al. correlation for R744 (Oritz et al., 2003), shown as below.

$$\eta_{\mathrm{tot}} = -0.26 + 0.7952\left(\frac{P_2}{P_1}\right) - 0.2803\left(\frac{P_2}{P_1}\right)^2 + 0.0414\left(\frac{P_2}{P_1}\right)^2 - 0.0022\left(\frac{P_2}{P_1}\right)^4 \tag{18}$$

$$\eta_{\mathrm{vol}} = 0.9207 - 0.0756\left(\frac{P_2}{P_1}\right) + 0.0018\left(\frac{P_2}{P_1}\right)^2 \tag{19}$$

For the gas cooler, under the cooling mode, the refrigerant is cooled by the ambient air and the water coming from the ground heat exchanger in series; while under the heating mode, the refrigerant is cooled by the water coming from the fan coils of the AHU. The pressure drop of R744 through the gas cooler is evaluated using a Darcy friction factor calculated by Blasius correlation (Blasius, 1913).

For the expansion valve, the model is denoted as:

$$h_{in} = h_{out} \tag{20}$$

For the evaporator, the thermal equilibrium equation is expressed as:

$$m_w Cp_w(T_{in} - T_{out}) = m_r(h_{1,r} - h_{4,r}) \tag{21}$$

3.4 Model validation

The models of the ground heat exchanger, the gas cooler and the heat pump system were validated, respectively. In the present study, the model validation for the ground heat exchanger was performed based on the experimental data in literature of Yang (2012), as shown in Fig. 4(a). The deviation of the predicted soil temperature to the experimental data is within ±0.2 ^{o}C. The model of the ambient air-cooled gas cooler was validated by the experimental data covering the operation conditions of the ambient temperatures from 25 ^{o}C to 45 ^{o}C and the inlet pressures of R744 in gas cooler from 75 Bar to 120 Bar, as shown in Table 1. The model deviations are within 10% (Fig. 4(b)). The model validation for the heat pump system was carried out with the experimental data of the system in Nevada and Wisconsin (USA) (Hackel and Pertzborn, 2011), and the maximum deviation of the temperature change predicted by the model is within 1 ^{o}C under the maximum load conditions, as shown in Fig. 4(c), meaning that the model's accuracy is sufficient for the investigation of the proposed R744 GSHP system.

4 Results and discussion

In order to compare the performance between the proposed R744 GSHP system and the existing system with other refrigerants, one archives building was used in the present study, which is in European style with the covered area of 8000 m^2, as the same in the existing research (Yang, 2012).

In the proposed R744 GSHP system, the heat pump system with the rated cooling capacity of 594 kW is used to power the air conditioning system, which has the similar energy loads with the building in the existing research (Yang, 2012). In order to decrease the influence of the adjacent ground heat exchangers, the distance between the boreholes was set as 4.0 m in the present study. The diameter of the borehole is 160 mm, and the shank spacing between the tubes is 80 mm, as the same in literature of Zhai et al. (2012); the depth of the boreholes is within 60 m ~ 200 m.

The performance and economy characteristics of the proposed R744 heat pump system will be analyzed under different climates. In the present study, the different climates in Shanghai and Guangzhou (China), New Delhi (India), and New Orleans (USA) were used for analyzing the effects of the climates on the system performance. The operation conditions of these cities are shown in Fig. 5. The soil temperature near the ground surface was directly related to the environmental temperature, while at depths of about 15 m the temperature is approximately constant and equal to the mean annual air temperature for different places (Rybach and Sanner, 2000); the ground temperature profiles can be estimated by applying Fourier's Law of heat conduction (Busby et al., 2009). The energy loads from TRNSYS 17.1 software (2012) were plugged into the system mathematic model as the input parameters.

Through the mathematic model of the system, the effects of indoor temperature, air cooling load proportion and the depth of the ground heat exchanger on the system performance were analyzed, and the detailed discussions were shown as below.

4.1 Effect of indoor temperature on earth's energy imbalance degree and system investment cost

Figure 6 shows the effect of the indoor temperature on the earth's energy imbalance degree and the investment cost of the proposed R744 system. It can be seen that, for the building under the climate in Shanghai (China), when the air cooling load proportion is 0%, the earth's energy imbalance degree initially decreases and then increases with the increasing indoor temperature, and the earth's energy imbalance degree will be close to zero when the indoor temperature is about 22 ^{o}C. This indoor temperature is feasible, somewhat low for some country, and then the air-cooled gas cooler is not needed.

With the increase of indoor temperature, the investment cost decreases initially and then keeps as constant. The reason is explained as below. As the setting indoor temperature increases, the cooling load of the air-cooled gas cooler decreases, and then the investment cost of air-cooled gas cooler decreases; while the investment cost of ground heat exchanger keeps as constant due to the certain heating load of the system, resulting in the decrease of investment costs with the increasing indoor temperature. As the setting indoor temperature further increases, the largest capacity of the air-cooled gas cooler lies on the highest environmental temperature, and the investment cost will be irrelevant to the setting indoor temperature, and the total investment cost will keep as constant.

With the increase of air cooling load proportion, the investment cost will be initially decreased and then increased. The reason is that, as the air cooling load proportion increases, the investment cost of the ground heat exchanger will be decreased, and the decrement is larger than the added cost of the ambient air-cooled gas cooler; when the air cooling load proportion is decreased to the value corresponding to the earth's energy balance condition, the investment cost of the ground heat exchanger reaches the lowest; with the further increase of the air cooling load proportion, the investment of the gas cooler increases while the investment of the ground heat exchanger keeps as a constant, resulting in the increase of the total investment with the increasing air cooling load proportion. The system COP increases with the increasing air cooling load proportion, but decreases with the increasing indoor temperature.

For the building under the climate in Guangzhou (China), there will be an earth's energy balance condition only when the air cooling load proportion is very large (80%). With the increase of the indoor temperature, the investment cost decreases, and the system COP decreases. While with the increase of the air cooling load proportion, the system COP increases under the higher air cooling load proportion conditions.

Therefore, the earth's energy imbalance degree and the investment cost can be decreased by adjusting the air cooling load proportion, and there must be a certain optimized value for the air cooling load proportion corresponding to the lowest earth's energy imbalance degree, the highest COP and the lowest cost, which will be analyzed in the next section.

4.2 Effect of air cooling load proportion on earth's energy imbalance degree, system investment cost and operation cost

The effect of the air cooling load proportion on the system performance is shown in Fig. 7. Under the climate in Shanghai (China), the air cooling load proportion for the energy balance condition is 45%, 29.5% and 4% for the indoor temperatures of 18 ^{o}C, 20 ^{o}C and 22 ^{o}C, respectively, and there will be no energy balance condition when the indoor temperature is up to 24 ^{o}C; while under the climate in Guangzhou (China), the air cooling capacity ratio for the energy balance condition is 95%, 90%, 82% and 71% for the indoor temperatures of 18 ^{o}C, 20 ^{o}C, 22 ^{o}C and 24 ^{o}C, respectively.

The investment cost, operation cost and the system COP for the earth's energy balance condition under the different operation conditions of indoor temperatures are also shown in Fig. 6. For the Shanghai (China) climate, the lowest investment cost corresponding to the earth's energy balance condition appears at the indoor temperature of 20 ^{o}C, and the air cooling load proportion under this condition is about 29.5%; the investment cost under the earth's energy balance condition is decreased by 12.6% comparing with that under the original system conditions without air-cooled gas cooler. For the Guangzhou (China) climate, the lowest investment cost corresponding to the earth's energy balance condition also appears at the indoor temperature of 20 ^{o}C, under which the system COP is larger than that under the higher temperature conditions.

The results show that, the earth's energy imbalance degree for the R744 heat pump system with the air-cooled and water-cooled gas coolers can be decreased to zero by adjusting the air cooling load proportion under the different climates, and the recommended indoor temperature for the Shanghai and Guangzhou (China) climates is about 20 ^oC. This recommended indoor temperature depends on the system specification and the operation conditions, and it may contain small match in consideration of wide operation conditions.

4.3 Effect of ground heat exchanger depth on the system performance

Figure 8 shows the effect of the ground heat exchanger depth on the system performance. With the increase of the ground heat exchanger depth from 60 m to 200 m, the total tube length needed for the system increases by 44%, and the system investment cost increases by 18%, meaning that the ground heat exchanger with shorter depth provides better performance of per unit length than that with longer depth. The possible reason is that, with the increase of the ground heat exchanger depth, the heat flux for per unit length decreases; for the same heat transfer capacity, with the increase of ground heat exchanger depth, the total tube length of the ground heat exchanger increases and thus the investment cost increases. The system COP will increase as the ground heat exchanger depth increases. The reason is that, with the increase of the ground heat exchanger depth, the temperature difference between the inlet and outlet tubes increases, and the evaporation temperature in the winter increases and the outlet temperature of R744 in the gas cooler in summer decreases, resulting in the increase of system COP.

4.4 Effect of climates on earth's energy imbalance degree, system investment cost and operation cost

Figure 9 shows the effect of climates on the system performance. The air cooling load proportions corresponding to the earth's energy balance conditions for climates in Shanghai (China), Guangzhou (China), New Delhi (India) and New Orleans (USA) are 29.5%, 90%, 62% and 84%, respectively; while the air cooling load proportions corresponding to the lowest investment conditions are around 20%~40%. The investment costs for the climates in Shanghai (China), Guangzhou (China) and New Orleans (USA) are almost same due to the similar highest cooling and heating loads, and are smaller than that for the climates in New Delhi (India) due to the lower cooling and heating loads.

Comparing with the original system without the air cooled-gas cooler, under the earth's energy balance conditions of the new system mentioned above, the investment cost for the climates in Shanghai (China), Guangzhou (China), New Delhi (India) and New Orleans (USA) decreases by 17.6%, 14.5%, 25.5% and 14.7%, respectively, and the operation cost decreases by 6.0%, 8.0%, 1.3% and 1.2%, respectively, resulting in the increase of the system COP.

The results can be deduced that, the R744 GSHP system with the ambient air-cooled and water-cooled gas coolers can be used under the hot climates to reduce the earth's energy imbalance degree. When the system is designed, the indoor temperature, the depth of ground heat exchanger and the operating power should be optimized for different climate regions.

4.5 Comparison between the proposed R744 GSHP system and the existing R134a system

Figure 10 shows the energy loads of the proposed R744 GSHP systems for every month under the condition of the earth's energy balance. Furthermore, the energy loads of the R744 GSHP system were compared with those of the existing R134a system in literature (Zhai and Yang, 2011; Yang, 2012).

Both the proposed R744 system and the existing R134a system are designed for the same achieves building, and they have the same ground heat exchanger and air handling unit (AHU). For the existing R134a GSHP system (Zhai and Yang, 2011; Yang, 2012), the compressor is a screw machine, and the power depends on the refrigerant flow rate, the evaporation pressure, the compression ratio and the isentropic compression coefficient (Yang, 2012); the type of heat pump system is Tran RTHDB2C2D2, which has the heat capacities of 594 kW and 610 kW for evaporator and condenser, respectively (Zhai and Yang, 2011); the ground heat exchanger consists of 280 vertical boreholes with the depth of 80 m and the diameter of 160 mm, and there is a single PE U-tube with the outer diameter of 32 mm in each borehole; all of the cooling loads in the system are undertaken by the ground heat exchanger. The detailed description on the R134a system GSHP can be referred to the literature (Zhai and Yang, 2011).

For the existing R134a system, the imbalance degrees for the climates in Shanghai (China), Guangzhou (China), New Delhi (India) and New Orleans (USA) are 29.5%, 90%, 62% and 84%, respectively. While for the proposed R744 GSHP system with the ambient air-cooled and water-cooled gas coolers, the cooling loads are undertaken by the ambient air and the water from the ground heat exchanger, and the energy imbalance degree can always be decreased to zero by adjusting the air cooling load proportion, as shown in Fig. 7.

Table 2 shows the comparison of the investment and operation costs between the R744 GSHP system and the existing R134a system. The investment cost of the R744 GSHP system is lower by 18%, 14%, 25.5% and 15% than those of the R134a systems for the climates in Shanghai (China), Guangzhou (China), New Delhi (India) and New Orleans (USA), respectively. The reason for the decreasing investment cost is that, by using the ambient air-cooled gas cooler in hot days, the maximum cooling load of the ground heat exchanger decreases (as shown in Fig. 10), and the amount of the ground heat exchanger decreases, resulting in the decrease of the system investment cost. The operation cost of the R744 GSHP system is 10%~17% larger than that of the original R134a system for different climates, but the total operation and investment costs of the R744 GSHP system is much lower than that of the original R134a system.

5 Conclusions

A R744 GSHP system with the ambient air-cooled and water-cooled gas coolers was designed for the building under different cooling dominated climates, which can provide the heating and cooling energy loads needed for the buildings by adjusting the air cooling load proportion. A numerical model for the proposed R744 system was developed to analyze the system performance, and the following results can be obtained:

1) The operation indoor temperature for the archives building under the different climates is recommended as 20 ^{o}C by considering the earth's energy imbalance degree, the system investment cost and the operation cost;
2) Comparing with the ground source heat pump system without the air-cooled gas cooler, the earth's energy imbalance degree for the R744 GSHP system with the air-cooled gas cooler in the different climates can always be decreased to zero through adjusting the air cooling load proportion, and the system investment cost for the climates in Shanghai (China), Guangzhou (China), New Delhi (India) and New Orleans (USA) can be decreased by 17.6%, 14.5%, 25.5% and 14.7%, respectively; while the operation costs can be decreased by 6.0%, 8.0%, 1.3% and 1.2%, respectively, resulting in the increase of the system COP;
3) For a certain heating or cooling load, as the ground heat exchanger depth increases from 60 m to 200 m, the total length of the ground heat exchanger increases by 44% due to the decrease of heat flux per meter, and the investment cost of the system increases by 18%. With the increase of ground heat exchanger depth, the heat flux for per unit length decreases, resulting in the increase of investment cost for a certain heat transfer capacity; therefore, the ground heat exchanger with shorter depth provides better performance of per unit length than that with longer depth due to the heat flux for per unit length decreases, and should be preferred in the ground source heat pump systems;
4) Comparing with the existing R134a ground source heat pump system, the application of R744 ground source heat pump system with the air-cooled and water-cooled gas coolers can always decrease the earth's energy imbalance degree to zero, and the system investment and operation costs can be decreased.

Acknowledgement

This publication forms a part of the SINTEF-NTNU CREATIV project, performed under the strategic

Norwegian research program RENERGI (195182/S60). The CREATIV is financially supported by the Research Council of Norway and several industry partners.

References

Abdelaziz, O., Shen, B., 2012. Cold climates heat pump design optimization. ASHRAE Transactions, 118(1), 34.

Abdelaziz, O., Shen, B., Gao, Z., Baxter, V. D., Iu, I., 2011. Development of a high performance air source heat pump for the US market. Oak Ridge National Laboratory (ORNL).

Aikins, K.A., Choi, J.M., 2012. Current status of the performance of GSHP (ground source heat pump) units in the Republic of Korea. Energy 47, 77-82.

Alavy, M., Nguyen, H.V., Leong, W.H., Dworkin, S.B., 2013. A methodology and computerized approach for optimizing hybrid ground source heat pump system design. Renewable energy 57, 404-412.

Austin, B.T., Sumathy, K., 2011a. Parametric study on the performance of a direct-expansion geothermal heat pump using carbon dioxide. Applied Thermal Engineering 31, 3774-3782.

Austin, B.T., Sumathy, K., 2011b. Transcritical carbon dioxide heat pump systems: A review. Renewable and Sustainable Energy Reviews 15, 4013-4029.

Bakirci, K., Colak, D., 2012. Effect of a superheating and sub-cooling heat exchanger to the performance of a ground source heat pump system. Energy 44, 996-1004.

Bakirci, K., Ozyurt, O., Comakli, K., Comakli, O., 2011. Energy analysis of a solar-ground source heat pump system with vertical closed-loop for heating applications. Energy 36, 3224-3232.

Bayer, P., Saner, D., Bolay, S., Rybach, L., Blum, P., 2012. Greenhouse gas emission savings of ground source heat pump systems in Europe: A review. Renewable and Sustainable Energy Reviews 16, 1256-1267.

Bi, Y.H., Guo, T.W., Zhang, L., Chen, L.G., 2004. Solar and ground source heat-pump system. Applied Energy 78, 231-245.

Blasius, H., 1913. Das Ähnlichkeitsgesetz bei Reibungsvorgängen in Flüssigkeiten. Springer Berlin Heidelberg.

Busby, J., Lewis, M., Reeves, H., Lawley, R., 2009. Initial geological considerations before installing ground source heat pump systems. Quarterly Journal of Engineering Geology and Hydrogeology 42(3), 295-306.

Capozza, A., Carli, M.D., Zarrella, A., 2012. Design of borehole heat exchangers for ground-source heat pumps: A literature review, methodology comparison and analysis on the penalty temperature. Energy and Buildings 55, 369-379.

Cavallini, A., Cecchinato, L., Corradi, M., Fornasieri, E., Zilio, C., 2005. Two-stage transcritical carbon dioxide cycle optimisation: a theoretical and experimental analysis. International Journal of Refrigeration 28, 1274-1283.

Choi, J., Kang, B., Cho, H., 2014. Performance comparison between R22 and R744 solar-geothermal hybrid heat pumps according to heat source conditions. Renewable Energy, 71, 414-424.

Dai, B.M., Li, M.X., Ma, Y.T., 2014. Thermodynamic analysis of carbon dioxide blends with low GWP (global warming potential) working fluids-based transcritical Rankine cycles for low-grade heat energy recovery. Energy 64, 942-952.

Dang, C.B., Hihara, E., 2012. Predicting the cooling heat transfer coefficient of supercritical CO_2 with a small amount of entrained lubricating oil by using the neural network method. International Journal of Refrigeration 25, 1130-1138.

Ge, Y.T., Cropper, R.T., 2009. Simulation and performance evaluation of finned-tube CO2 gas coolers for refrigeration systems. Applied Thermal Engineering 29, 957-965.

Jeon, J., Lee, S., Hong, D., Kim, Y., 2010. Performance evaluation and modeling of a hybrid cooling system combining a screw water chiller with a ground source heat pump in a building. Energy 35, 2006-2012.

Jiang, P.X., Zhang, Y., Zhao, C.R., Shi, R.F., 2008. Convection heat transfer of CO2 at supercritical pressures in a vertical mini tube at relatively low Reynolds numbers. Experimental Thermal and Fluid Science 32, 1628-1637.

Hackel, S., Pertzborn, A., 2011. Effective design and operation of hybrid ground-source heat pumps: Three case studies. Energy and Buildings 43, 3497-3504

Han, Z., Zheng, M., Kong, F., Wang, F., Li, Z., Bai, T., 2008. Numerical simulation of solar assisted ground-source heat pump heating system with latent heat energy storage in severely cold area. Applied Thermal Engineering 28, 1427-1436.

Li, S.S., Li, S.H., Zhang, X.S., 2015. Simulation research of a hybrid heat source heat pump using R134a, R744 instead of R22 for domestic water heating in residential buildings. Energy and Buildings 91: 57-64.

Liu, J., Zhang, X., Gao, J., Yang, J., 2009. Evaluation of heat exchange rate of GHE in geothermal heat pump systems. Renewable energy 34, 2898-2904.

Lund, J.W., Freeston, D.H., Boyd, T.L., 2011. Direct utilization of geothermal energy 2010 worldwide review. Geothermics, 40(3), 159-180.

Ma, Y., Liu, Z., Tian, H., 2013. A review of transcritical carbon dioxide heat pump and refrigeration cycles. Energy 55, 156-172.

Madani, H., Claesson, J., Lundqvist, P., 2013. A descriptive and comparative analysis of three common control techniques for an on/off controlled Ground Source Heat Pump (GSHP) system. Energy and Buildings, 65, 1-9.

Man, Y., Yang, H.X., Wang, J.G., 2010. Study on hybrid ground-coupled heat pump system for air-conditioning in hot-weather areas like Hong Kong. Appl. Energ. 87, 2826-2833.

METEOTEST, 2006. METEONORM Version 5.1x. Switzerland.

Nekså, P., 2002. CO_2 heat pump systems. International Journal of refrigeration 25, 421-427.

Omer, A.M., 2008. Energy environment and sustainable development. Renew Sustain Energy Rev 12, 2265-2300.

Oritz, T.M., Li, D., Groll, E.A., 2003. Evaluation of the performance potential of CO_2 as a refrigerant in air-to-air air conditioners and heat pumps: System modeling and analysis. ARTI, Final Report.

Ozgener, O., Hepbasli, A., 2007. A parametrical study on the energetic and exergetic assessment of a solar-assisted vertical ground-source heat pump system used for heating a greenhouse. Building and Environment 42, 11-24.

Ozgener, O., Hepbasli, A., 2005a. Performance analysis of a solar-assisted ground-source heat pump system for greenhouse heating: an experimental study. Building and Environment 40, 1040-1050.

Ozgener, O., Hepbasli, A., 2005b. Experimental performance analysis of a solar assisted ground-source heat pump greenhouse heating system. Energy and Buildings 37, 101-110.

Qi, Z., Gao, Q., Liu, Y., Yan, Y.Y., Spitler, J.D., 2014. Status and development of hybrid energy systems from hybrid ground source heat pump in China and other countries. Renewable and Sustainable Energy Reviews 29, 37-51.

Rad, F.M., Fung, A. S., Leong, W. H., 2013. Feasibility of combined solar thermal and ground source heat pump systems in cold climate, Canada. Energy and Buildings 61, 224-232.

Richter, M.R., Song, S.M., Yin, J.M., Kim, M.H., Bullard, C.W., Hrnjak, P.S., 2003. Experimental results of transcritical CO_2 heat pump for residential application. Energy 28, 1005-1019.

Rybach, L., Sanner, B., 2000. Ground source heat pump systems, the European experience. GHC Bulletin 21, 16-26.

Sagia, Z., Rakopoulos, C., Kakaras, E., 2012. Cooling dominated hybrid ground source heat pump system application. Applied Energy 94, 41-47.

Shen B., Abdelaziz O., Rice K., 2012. Auto-calibration and control strategy determination for a variable-speed heat pump water heater using optimization. HVAC&R Research 18(5): 904-914.

Si, Q., Okumiya, M., Zhang, X., 2014. Performance evaluation and optimization of a novel solar-ground source heat pump system. Energy and Buildings 70, 237-245.

Tarnawski, V.R., Leong, W.H., Momose, T., Hamada, Y., 2009. Analysis of ground source heat pumps with horizontal ground heat exchangers for northern Japan. Renewable Energy 34, 127-134.

TRNSYS 17.1, 2012. TRNSYS A transient systems simulation program. http://sel.me.wisc.edu/trnsys.

Wang, C.C., Jang, J.Y., Chiou, N.F., 1999. A heat transfer and friction correlation for wavy fin-and-tube heat exchangers, Int. J. Heat and Mass Transfer 42, 1919-1924.

Wang, E., Fung, A.S., Qi, C., Leong, W.H., 2012. Performance prediction of a hybrid solar ground-source heat pump system. Energy and Buildings 47, 600-611.

Wang, H.J., Qi, C.Y., Wang, E.Y., Zhao, J., 2009. A case study of underground thermal storage in a solar-ground coupled heat pump system for residential buildings. Renewable Energy 34, 307-314.

Wang, S., He, Y., Tuo, H., Cao, F. Xing, Z., 2013. Effect of heat transfer area and refrigerant mass flux in a gas cooler on heating performance of air-source transcritical CO2 heat pump water heater system. Energy and Buildings 67, 1-10.

Xu, X.X., Chen, G.M., Tang, L.M., Zhu, Z.J., 2012. Experimental investigation on performance of transcritical CO_2 heat pump system with ejector under optimum high-side pressure. Energy 44, 870-877.

Yang, C.Y., Xu, J.L., Wang, X.D., Zhang, W., 2013. Mixed convective flow and heat transfer of supercritical CO_2 in circular tubes at various inclination angles. International Journal of Heat and Mass Transfer 64, 212-223.

Yang, H., Cui, P., Fang, Z., 2010. Vertical-borehole ground-coupled heat pumps: a review of models and systems. Appl. Energ. 87, 16-27.

Yang, Y., 2012. Optimization and application research of constant temperature and humidity of air-conditioning system driven by ground source heat pumps. Master thesis. Shanghai Jiao Tong University.

Yu, X., Zhai, X.Q. Wang, R.Z., 2010a. Design and performance of a constant temperature and humidity air-conditioning system driven by ground source heat pumps in winter. Energy Conversion and Management 51, 2162-2168.

Yu, X., Zhai, X.Q. Wang, R.Z., 2010b. Design and Performance of a Constant Temperature and Humidity Air-Conditioning System Driven by a Ground Source Heat Pump in Summer. ASME Journal of Thermal Science and Engineering Applications 2, 014502.

Yuan, Y., Cao, X., Sun, L., Lei, B., Yu, N., 2012. Ground source heat pump system: A review of simulation in China. Renewable and Sustainable Energy Reviews 9, 6814-6822.

Zeng, H.Y., Diao, N.R., Fang, Z.H., 2002. A finite line-source model for boreholes in geothermal heat exchangers. Heat Transfer-Asian Research 31, 558-567.

Zeng, H.Y., Diao, N.R., Fang, Z.H., 2003. A quasi three dimensional heat transfer model for vertical U-tube geothermal heat exchangers. J. Eng. Therm. Energ. Power 18, 387-390.

Zhai, X.Q., Qu, M., Yu, X., Yang, Y., Wang, R.Z., 2011. A review for the applications and integrated approaches of ground-coupled heat pump systems. Renewable and Sustainable Energy Reviews 15, 3133-3140.

Zhai, X.Q., Wang, X.L., Pei, H.T., Yang, Y., Wang, R.Z., 2012. Experimental investigation and optimization of a ground source heat pump system under different indoor set temperatures. Applied Thermal Engineering 48, 105-116

Zhai, X.Q., Yang, Y., 2011. Experience on the application of a ground source heat pump system in an archives building. Energy and Buildings 43, 3263-3270.

Zhang, W.Y., Wei, J., 2012. Analysis on the soil heat accumulation problem of ground source heat pump system in high temperature and high humidity areas. Energy Procedia 14, 198-204.

Zhang, X.R., Yamaguchi, H., 2007. Forced convection heat transfer of supercritical CO_2 in a horizontal circular tube. The Journal of supercritical fluids 41, 412-420.

Fig. 1 Schematic diagram for subcritical and transcritical refrigeration cycles

Fig. 2 Schematic diagram of R744 ground source heat pump system with air-cooled and water-cooled gas coolers

Fig. 3 Single control volume segment of gas cooler

Fig. 4 Model validation for the ground source heat pump system with air-cooled and water-cooled gas coolers

Fig. 5 Effect of indoor temperature on earth's energy imbalance and investment cost of the proposed R744 system

Fig. 6 Climates for different cities in different countries

Fig. 7 Effect of cooling load proportion of air-cooled gas cooler on the R744 system performance

Fig. 8 Effect of depth of ground heat exchanger on the system performance

Fig. 9 Effect of climates on the R744system performance

Fig. 10 Comparison of energy load between different heat pump systems

Table 1 The performance of ambient air-cooled gas cooler

Ambient Temp. ^{o}C	Inlet Pres. Bar	Inlet Temp. ^{o}C	Outlet Temp. ^{o}C	Mass Flow of R744 kg h^{-1}	Pressure Drop of R744 Bar	Exp. heat capacity kW	Predicted heat capacity kW
25	75	88	27	2641.54	0.03	171	187
25	75	88	25.4	2565.98	0.028	171	161
30	78.5	88	32	6046.27	0.12	342	362
30	78.5	88	30.4	5704.51	0.11	342	331
35	92	88	37	11184.38	0.3	570	583
45	85	88	47	30857.14	237	395	370
45	120	88	47	11074.29	50	240	258
45	120	140	45.4	18120	38	335	319

Table 2 Comparison of investment and operation costs between different systems

Climate	Investment cost (10^4 CNY)		Operation cost (10^4 CNY)	
	R134a system	R744 system	R134a system	R744 system
Shanghai (China)	316.23	260.32	35.25	38.2
Guangzhou (China)	319.03	272.82	37.39	38.12
New Delhi (India)	372.77	277.51	45.45	37.83
New Orleans (USA)	321.16	270.00	55.39	58.92